# Electron-microscopic demonstration of multidrug resistance protein 2 (Mrp2) retrieval from the canalicular membrane in response to hyperosmolarity and lipopolysaccharide

Frank DOMBROWSKI*, Ralf KUBITZ†, Anila CHITTATTU*, Matthias WETTSTEIN†, Nirmalendu SAHA†[1] and Dieter HÄUSSINGER†[2]

*Department of Pathology, Bonn University, Bonn, Germany, and †Clinic for Gastroenterology, Hepatology and Infectiology, Heinrich-Heine-University, Düsseldorf, Germany

Immunohistochemical studies suggest that canalicular secretion via multidrug resistance protein 2 (Mrp2), a conjugate export pump encoded by the *Mrp2* gene, is regulated by rapid transporter retrieval from/insertion into the canalicular membrane. The present study was undertaken in order to investigate this suggestion by means of immunogold electron microscopy. Therefore the effects of lipopolysaccharide (LPS) and osmolarity on Mrp2 localization were studied following immunogold labelling in the perfused rat liver by quantitative electron microscopy and morphometric analyses, and by confocal laser scanning microscopy. Mrp2 activity was assessed in the isolated perfused rat liver by measuring the excretion of dinitrophenyl-S-glutathione as a substrate of Mrp2. Both LPS and hyperosmolarity resulted in a statistically significant decrease in immunogold-labelled Mrp2 in the canalicular membrane and canalicular villi, and an increase in labelling in the pericanalicular cytoplasm. Canalicular morphometric parameters were unchanged under these conditions compared with controls. Under hyperosmolar perfusion Mrp2, but not the canalicular protein dipeptidylpeptidase IV, was found inside the cells, as shown by double immunofluorescence and confocal laser scanning microscopy. The findings suggest a selective retrieval of Mrp2 from the canalicular membrane under the influence of hyperosmolarity and LPS, whereas canalicular morphology remains unchanged.

Key words: ABC-transporter, cell volume, electron microscopy, lipopolysaccharide.

## INTRODUCTION

Canalicular secretion of glutathione and glucuronide conjugates is accomplished by multidrug resistance protein 2 (Mrp2), a conjugate export pump encoded by the *Mrp2* gene [1–9]. Long-term regulation of Mrp2 occurs at the level of gene expression and involves regulation by glucocorticoids, lipopolysaccharide (LPS) and osmolarity [10–12]. On the other hand, these effectors also control Mrp2 function on a short-term basis, at the level of transporter insertion into and retrieval from the canalicular membrane [11,13], as shown by immunohistochemistry and confocal laser scanning microscopy. Hyperosmotic exposure [13], LPS [11] or phalloidin [14] resulted in the appearance of immunoreactive Mrp2 in a subcanalicular compartment, suggestive of rapid transporter retrieval from the canalicular membrane and generation of cholestasis. Evidence has been obtained that the Mrp2 transporter, once retrieved from the canalicular membrane under the influence of hyperosmolarity, has the potential for re-insertion into the membrane following hypo-osmotic re-exposure [13].

In view of the importance of the dynamic equilibrium between transporter retrieval and insertion for understanding of the pathogenesis of cholestasis, confirmation of the findings obtained by immunohistochemistry and confocal laser scanning microscopic using an independent technique was desirable. It was also important to determine whether retrieval of Mrp2 due to hyperosmolarity or LPS exposure is accompanied by a change in the canalicular membrane surface. In the present study, immunogold labelling, electron microscopy and quantitative assessment was used as another technique in order to study the subcellular distribution of Mrp2 under the influence of LPS and anisosmolarity. The data show that retrieval of Mrp2 under these conditions occurs in the absence of gross changes in canalicular morphology.

## MATERIALS AND METHODS

### Materials

The EAG15 polyclonal antibody was raised against the 12-amino-acid peptide sequence at the C-terminus of the rat Mrp2 sequence, as described in [6], and was generously donated by Professor Dr D. Keppler (Deutsches Krebsforschungszentrum, Heidelberg, Germany). Rat anti-(mouse ZO-1) (where ZO-1 is zona occludens protein-1, part of the tight-junction complex) [15] was from Biozol (Eching, Germany). The monoclonal antibody MAB 13.4 was raised against dipeptidylpeptidase IV (Dpp IV) [16] and was a gift from Professor Dr W. Reutter (Freie Universität, Berlin, Germany). Cy3-conjugated AffiniPure® goat anti-rabbit IgG (H + L), FITC-conjugated goat anti-rat IgG (H + L) and gold-conjugated goat anti-rabbit antibody (10 nm gold particles) were from Jackson ImmunoResearch Laboratories (West Grove, PA, U.S.A.). FITC-conjugated goat anti-mouse IgG (H + L) was from Southern Biotechnology Associates (Birmingham, AL, U.S.A.). All other chemicals were of highest purity and were purchased from Fluka (Neu-Ulm, Germany) or Aldrich (Steinheim, Germany).

Abbreviations used: CDNB, 1-chloro-2,4-dinitrobenzene; Dpp IV, dipeptidylpeptidase IV; GS-DNP, dinitrophenyl-S-glutathione; KHB, Krebs/Henseleit buffer; LPS, lipopolysaccharide; Mrp2, multidrug resistance protein 2; ZO-1, zona occludens protein-1.

[1] Present address: Department of Zoology, North-Eastern Hill University, Shillong, India.

[2] To whom correspondence should be addressed: Klinik für Gastroenterologie, Hepatologie und Infektiologie, Heinrich-Heine-Universität, Moorenstrasse 5, 40225 Düsseldorf, Germany (e-mail haeussin@uni-duesseldorf.de).

**Table 1 Electron-microscopic analyses of Mrp2 distribution in aniso-osmolar perfused and LPS-treated rat liver**

Gold particles (marking Mrp2) attached to the bile canalicular membrane ($g_{bcm}$) or located in the cytosol ($g_{cyt}$) within 1 $\mu$m around the canaliculi were counted as described in the Materials and methods section. The amount of Mrp2 attached to the canalicular membrane was significantly reduced in livers undergoing hyperosmolar (405 mosmol/l) perfusion and in livers from LPS-treated rats. The relative amount of gold-marked Mrp2 attached to the canalicular membrane [$g_{bcm}/(g_{bcm}+g_{cyt})$] was significantly different between livers undergoing hypo- and hyper-osmolar perfusion, as well as between livers from LPS-treated rats and all other conditions (perfusion of livers from control rats at 205, 305 or 405 mosmol/l). Morphometric analyses revealed no differences in the relative area of the bile canalicular membrane ($Area_{bcm}$) or in the relative pericanalicular volume ($Vol_{cyt}$) between all conditions. When the amounts of gold particles were standardized to the canalicular membrane area and the pericanalicular volume (see the Materials and methods section), the distribution of Mrp2 between the canalicular membrane and the pericanalicular cytoplasm [$R_{bcm}/R_{cyt} = (g_{bcm}/Area_{bcm})/(g_{cyt}/Vol_{cyt})$] is changed significantly in favour of a cytoplasmic localization in livers undergoing hyperosmolar perfusion or from LPS-treated rats. Significance of differences: $^*P < 0.05$ compared with perfusion at 205 mosmol/l; †$P < 0.05$ compared with perfusion at 205 and 305 mosmol/l; ‡$P < 0.05$ compared with perfusion at 205, 305 and 405 mosmol/l.

| Condition (*n*) | $g_{bcm}$ | $g_{cyt}$ | $g_{bcm}/(g_{bcm}+g_{cyt})$ | $Area_{bcm}$ | $Vol_{cyt}$ | $R_{bcm}/R_{cyt}$ |
|---|---|---|---|---|---|---|
| Perfusion at 205 mosmol/l (8) | 4.5 ± 0.6 | 4.0 ± 0.4 | 0.53 ± 0.04 | 19.7 ± 1.3 | 64.9 ± 1.8 | 4.3 ± 0.8 |
| Perfusion at 305 mosmol/l (7) | 4.1 ± 0.8 | 5.2 ± 1.3 | 0.45 ± 0.04 | 21.5 ± 1.8 | 65.1 ± 3.2 | 2.6 ± 0.3 |
| Perfusion at 405 mosmol/l (8) | 2.9 ± 0.5* | 5.0 ± 0.8 | 0.37 ± 0.01* | 21.1 ± 1.4 | 63.7 ± 2.9 | 1.8 ± 0.1*† |
| LPS treatment (6) | 1.7 ± 0.2‡ | 4.8 ± 0.6 | 0.26 ± 0.03‡ | 22.9 ± 4.9 | 57.9 ± 3.1 | 1.0 ± 0.2‡ |

### Rat liver perfusion

The experiments were approved by the relevant local authorities. Livers were obtained from male Wistar rats (120–150 g) that had had free access to stock diet and tap water, and were perfused *in situ* in a non-recirculating system with Krebs/Henseleit Buffer (KHB; 305 mosmol/l) at 37 °C, equilibrated with 5 %/95 % $CO_2/O_2$ and supplemented with 0.3 mmol/l pyruvate and 2.1 mmol/l lactate, as described previously [17–19]. The liver weight was estimated to be 4 % of the body weight. The perfusate flow rate was approx. 4 ml/min per g of liver, and was kept constant throughout the individual experiments. Potassium and pH were monitored continuously with electrodes (Radiometer, Copenhagen, Denmark). Portal pressure was recorded using a pressure transducer (Hugo Sachs Electronics, March, Germany). Bile ducts were cannulated and samples were collected every 2 min. 1-Chloro-2,4-dinitrobenzene (CDNB; 10 $\mu$mol/l) was added to the influent perfusate using precision micropumps. Dinitrophenyl-S-glutathione (GS-DNP; the glutathione conjugate of CDNB) was determined photometrically at 334 nm in bile and in the effluent, as described in [20,21]. The osmolarity of the perfusion buffer was changed from 305 mosmol/l to 205 or 405 mosmol/l by the appropriate removal or addition of NaCl.

### Sectioning and staining for electron-microscopic analyses of Mrp2

Livers from rats treated with LPS 12 h prior to the experiment were perfused for 5 min with normo-osmolar (305 mosmol/l) KHB in order to remove blood. After this the livers were perfusion-fixed with 3 % paraformaldehyde plus 0.2 % glutaraldehyde. Livers from untreated rats were perfused for 20 min with normo-osmolar KHB and for another 30 min with normo-osmolar (305 mosmol/l), hypo-osmolar (205 mosmol/l) or hyperosmolar (405 mosmol/l) KHB before fixation.

After fixation, small cubes of dimensions 0.5 mm × 0.5 mm × 0.5 mm were cut with a razor blade. Four cubes per liver were embedded into Lowicryl K4M (Polysciences, Warrington, PA, U.S.A.) as follows. After dehydration with increasing concentrations of ethanol [30 % (v/v) for 30 min at 4 °C; 50 % for 1 h at 4 °C; 70 % for 1 h at 4 °C; 90 % for 1 h at −35 °C; 100 % for 1 h at −35 °C], the cubes were embedded in increasing concentrations of Lowicryl [Lowicryl/ethanol (1:1, v/v) for 20 h at −35 °C; Lowicryl/ethanol (2:1) for 24 h at −35 °C; pure Lowicryl for 24 h at −35 °C], followed by polymerization under UV light (24 h at −35 °C and 72 h at 21 °C). Thin sections were prepared from two tissue blocks from every liver with an ultramicrotome system ('2128 ultrotome'; LKB). Sections were placed on a carbon-filmed 200-mesh 3 mm copper grid (Plano, Wetzlar, Germany).

Immunohistochemistry was performed as follows. Aldehyde moieties were blocked with 0.05 mol/l glycine in PBS (0.1 mol/l, pH 7.6, 21 °C) for 15 min. Thereafter, unspecific protein binding was blocked by incubation with 5 % (v/v) normal goat serum plus 5 % (w/v) BSA plus 0.1 % cold washed fish gelatin (Aurion, Amsterdam, The Netherlands) in PBS for 30 min. Slides were washed three times for 5 min (0.1 % BSA in PBS), and the primary antibody (anti-Mrp2 = EAG15; dilution 1:500) was applied for 1 h. After a second washing procedure the tissue sections were incubated for 2 h with the secondary goat anti-rabbit antibody conjugated to gold particles (dilution 1:20). A final washing, including a short fixation with 2 % glutaraldehyde in PBS for 10 min, was followed by incubation with 2 % uranyl acetate for 5 min and 1.5 % lead citrate for 5 s to provide the contrast.

### Morphometric analyses of electron-microscopic pictures

Morphometric analyses were carried out as described in [22]. Analyses of the data were performed in a 'blinded' way to exclude bias by the investigator. The thin sections were viewed with a CM10 electron microscope (Phillips, Eindhoven, The Netherlands). The open squares of the copper grid were taken as test fields. Fields in acinar zone 2 were chosen at a low magnification (× 700). The quality of the immunohistochemistry was checked for every test field, and fields with a background staining over mitochondria, nuclei or sinusoids were excluded. From six test fields for each section, micrographs were randomly taken at primary magnifications of × 8900 and × 15500. Photo prints were enlarged to final magnifications of × 23000 and × 40000. Typically, no or only sparse gold dots were found outside a zone of 1 $\mu$m around the bile capillary. Therefore lines at a distance of 4 cm around the bile capillaries (representing the hepatocytic cytoplasm within a distance of 1 $\mu$m from the bile capillary) were drawn by hand on the photo prints at × 40000. The gold dots on the hepatocytic cytoplasm within the area bordered by the drawn line ($g_{cyt}$) and the gold dots on the membrane of the bile capillary membrane ($g_{bcm}$) were counted separately.

A square point lattice system consisting of 12 lines and 144 points was superimposed. The points lying over the hepatocytic cytoplasm inside the drawn line were counted. They reflect a relative measure of the pericanalicular volume of the hepatocytic

cytoplasm at a distance of 1 $\mu$m around the bile capillary ($Vol_{cyt}$) [22]. The points where the parallel lines cut the bile capillary membrane (including all cuts of the microvilli) were counted. They represent a measure of the relative surface area of the bile capillary ($Area_{bcm}$) [22]. The ratio $R_{cyt}$ ($= g_{cyt}/Vol_{cyt}$) represents the relative number of gold dots in the hepatocytic cytoplasm within 1 $\mu$m around the bile capillary. The ratio $R_{bcm}$ ($= g_{bcm}/Area_{bcm}$) represents the relative number of gold dots on the bile capillary membrane. The relationship of these two ratios ($R_{bcm}/R_{cyt} = D_{b/c}$) was the target value in this study. It represents the distribution of Mrp2 between the canalicular membrane and the pericanalicular cytoplasm.

### Cryosectioning and immunostaining of rat liver for evaluation of Mrp2 by confocal laser microscopy

Livers were perfused with normo-osmotic KHB for 20 min. A liver lobe was ligated, excised and frozen in isopentane precooled in liquid nitrogen. Thereafter, the osmolarity was changed to 205 or 405 mosmol/l, or left at 305 mosmol/l. After 30 and 60 min a second and third lobe respectively was excised and frozen. The tissue samples were cryosectioned and stained for Mrp2 (EAG15 antibody; 1:5000), DppIV (MAB13.4 antibody; 1:3) or ZO-1 (1:500) according to standard protocols described in detail in [11].

### Aquisition of pictures by confocal laser scanning microscopy

Immunostained rat liver tissue samples were analysed using a Leica TCS-NT confocal laser scanning system with an argon/krypton laser on a Leica DM IRB inverted microscope. Images were acquired from two channels at excitation wavelengths of 488 nm and 568 nm. Emission was measured at $530 \pm 10$ nm (green) and $> 590$ nm (red). Co-localization of the green (fluorescein) and red (Cy3) fluorescent dyes results in a yellow signal. Only samples that were prepared in parallel in all steps were compared, using the same adjustments for all parameters (i.e. laser power, filter settings, setting of the acousto–optical tunable filter, pinhole, lens, voltages at the photomultiplier tubes, number of accumulated scans, format size and zoom, scan speed and z-step-size).

### Statistics

Data are expressed as means $\pm$ S.E.M. ($n$ = number of livers studied). Results were compared by Students $t$-test, and $P < 0.05$ was considered statistically significant.

## RESULTS AND DISCUSSION

### Effects of ambient osmolarity and LPS on the distribution of Mrp2

Rat livers were exposed for 30 min to normo- or aniso-osmolar perfusion medium, or rats were pretreated with a single intraperitoneal LPS injection 12 h prior to the perfusion experiment. Morphometric analyses of electron-microscopic pictures of these livers revealed that neither anisotonicity nor LPS pretreatment had an effect on the pericanalicular volume ($Vol_{cyt}$), the bile canalicular membrane surface area ($Area_{bcm}$) (Table 1) or the canalicular volume (results not shown). Thus neither aniso-osmolar perfusion nor LPS treatment had any effect on the morphometric characteristics of the (peri-) canalicular area. In contrast, the absolute amount of gold-particle-labelled Mrp2 ($g_{bcm}$) and the relative amount of Mrp2 [$g_{bcm}/(g_{bcm}+g_{cyt})$] localized at the bile canalicular membrane was significantly decreased after 30 min of hyperosmolar (405 mosmol/l) perfusion when compared with a 30 min perfusion with hypo-osmolar (205 mosmol/l) medium (Table 1), while the total amount of Mrp2 ($g_{bcm}+g_{cyt}$) under these conditions was not statistically different (results not shown). Representative electron-microscopic pictures for the normo- and hyper-osmotic conditions are shown in Figures 1(A) and 1(B).

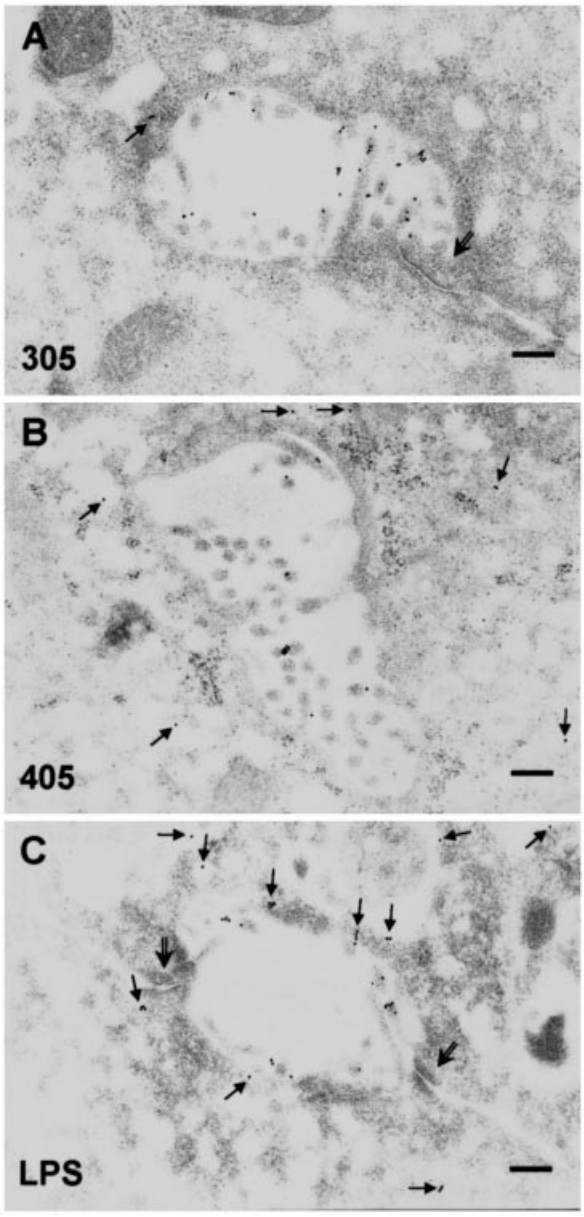


**Figure 1 Localization of Mrp2, as determined by electron microscopy**

Rat livers were perfused with (**A**) normo-osmotic (305 mosmol/l) or (**B**) hyperosmotic (405 mosmol/l) medium, or livers were obtained from rats that had been treated with LPS 12 h prior to fixation (**C**). Liver sections were stained by the immunogold method, as described in the Materials and methods section. Under normo-osmotic conditions, most immunogold-labelled Mrp2 molecules are attached to the canalicular membrane, and a small amount of Mrp2 is found inside the cells (**A**). Under hyperosmotic conditions, more Mrp2 is found inside the cells away from the canaliculus (**B**). In LPS-treated livers most of the gold-particle-labelled Mrp2 is found inside the cells, i.e. the distribution of Mrp2 between cytosol and canaliculus is reversed in favour of the cytosol (**C**) compared with controls (**A**). $\rightarrow$, Gold particle(s) inside the cell; $\Rightarrow$, tight junctions. Bars = 0.25 $\mu$m.

The absolute ($g_{bcm}$) and relative [$g_{bcm}/(g_{bcm}+g_{cyt})$] decreases in the amount of immunoreactive Mrp2 in the canalicular mem-

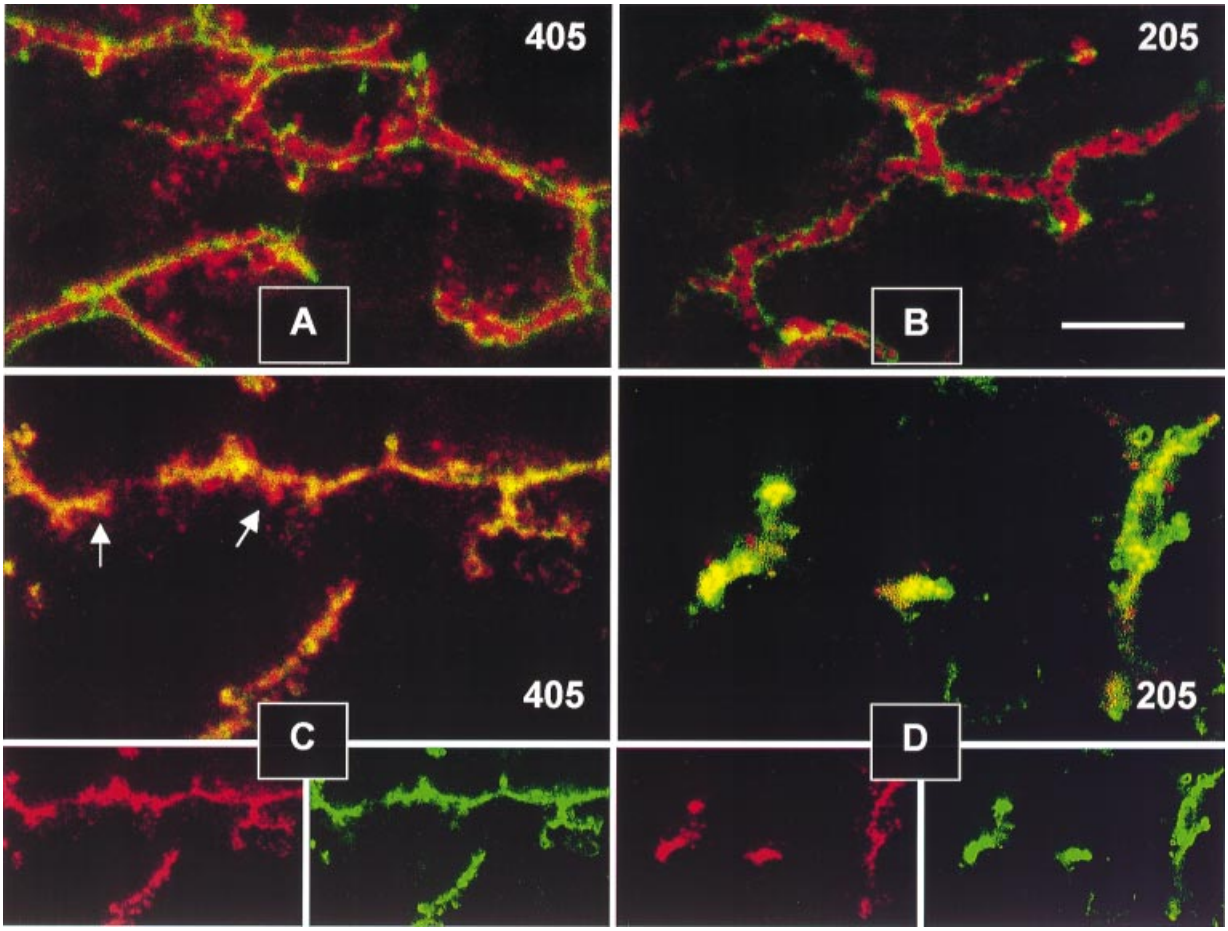


**Figure 2 Hyperosmolarity-induced retrieval of Mrp2 is reversible and selective, as determined by immunohistochemistry**

(**A**, **B**) Rat livers were perfused with hyperosmolar buffer (405 mosmol/l; **A**), shock frozen, cryosectioned and then immunostained for Mrp2 (red). Under these conditions Mrp2 is found partly outside the canalicular domain, as delineated by the tight-junction protein ZO-1 (green). When perfusion is continued with hypo-osmolar buffer (205 mosmol/l; **B**) most of the immunoreactive Mrp2 is relocalized in the canalicular membrane, as is the case under normal conditions (not shown). (**C**, **D**) Mrp2 (red), but not DppIV (green), is found at a distance from the canaliculi in livers perfused with hyperosmolar medium (405 mosmol/l; **C**), while Mrp2 and Dpp IV are largely co-localized when perfusion is continued with hypo-osmolar medium (205 mosmol/l; **D**). Large pictures show co-localization, whereas small pictures show single channels. Bar = 10 $\mu$m.

brane under the influence of LPS (Figure 1C) were even more pronouced than those obtained under hyperosmotic conditions (Figure 1B). Both values were statistically different compared with all three conditions of short-term perfusion with KHB at 205, 305 and 405 mosmol/l (Table 1). The decrease in total Mrp2 ($g_{bcm} + g_{cyt}$) may reflect both the LPS-induced down-regulation of Mrp2 at the level of mRNA and protein expression [10,11] and Mrp2 translocation into areas of the cellular interior that were not covered by the areas of interest for electron-microscopic morphology (Figure 1C; compare with Figures 4 and 6 in [11]). The relative distribution of Mrp2 between canalicular membrane and cytosol was shifted in favour of the cytosol by LPS (i.e. only 26 % of gold-labelled Mrp2 was found in the canalicular membrane). Thus retrieval of Mrp2 from the canalicular membrane might explain the highly asymmetrical distribution of Mrp2 under these conditions. Further, this redistribution corresponds well with the observed appearance of immunoreactive Mrp2 inside the cells of LPS-treated livers, as shown by confocal laser scanning microscopy [11].

The fraction of Mrp2 in the bile canalicular membrane was reduced to 57 % in livers from LPS-treated rats compared with normo-osmotic control livers (305 mosmol/l perfusion) (Table 1; $0.26/0.45 = 0.57$). This agrees well with the observed decrease in the excretion of bromosulphalein-glutathione (another tracer of Mrp2 [23]) in perfused rat liver, which was present at 58 % of control values 12 h after LPS injection.

The ratio $R_{bcm}/R_{cyt}$ [$= (g_{bcm}/Area_{bcm})/(g_{cyt}/Vol_{cyt})$] reflects the distribution of Mrp2 between the canalicular membrane and the cytosol under consideration of canalicular membrane area and pericanalicular volume. Hyperosmotic perfusion led to a significant shift of Mrp2 from the canaliculus into the cytosol when compared with normo- and hypo-osmolar perfusion (Table 1). Under hypo-osmotic conditions a tendency for Mrp2 to become more attached to the canalicular membrane was seen; however, statistical significance was not reached. This observation is in line with data from a confocal laser microscopy study [13] showing that the fluorescence profile of Mrp2 distribution under hypo-osmolar perfusion is 'sharper', but not statistically different from that under normo-osmotic conditions. These data confirm that hyperosmotic cell shrinkage leads to a redistribution of Mrp2 from the canalicular membrane to the cytosol [13].

With the high resolution of electron microscopy, it became apparent that under control conditions (normo-osmotic per-

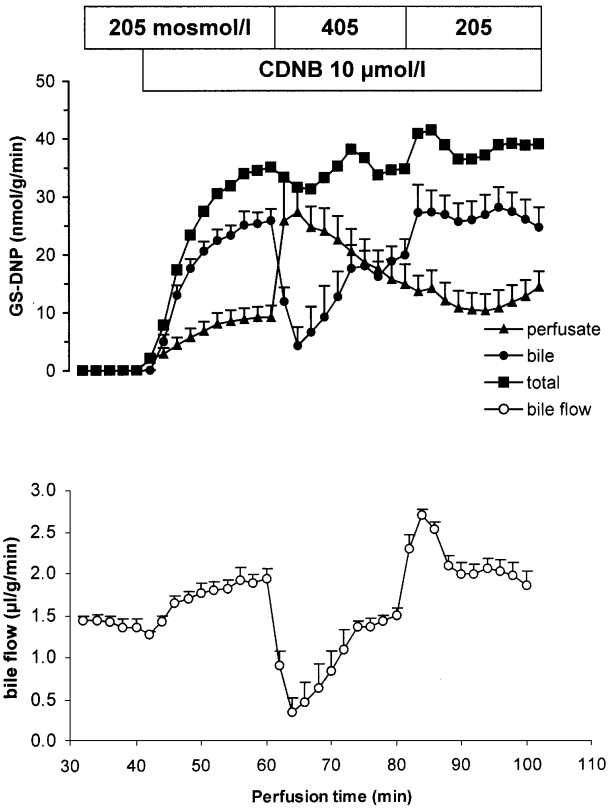


**Figure 3 The hyperosmolarity-induced down-regulation of Mrp2 activity is reversible in the isolated perfused rat liver**

The change from a hypo-osmolar (205 mosmol/l) to a hyperosmolar (405 mosmol/l) perfusion buffer significantly reverses the relationship of the biliary (●) and sinusoidal (▲) release of GS-DNP in the perfused rat liver, while total GS-DNP excretion (■) remains almost constant. Livers were first perfused with hypo-osmolar (205 mosmol/l) KHB, then for 20 min with hyperosmolar (405 mosmol/l) KHB, and then again with hypo-osmolar KHB. CDNB (10 $\mu$mol/l) was added to the influent perfusate and the concentrations of its glutathione conjugate, GS-DNP, were determined in bile and effluent perfusate. Values are means + S.E.M. ($n = 5$).

fusion) approx. one-half of the immunoreactive Mrp2 resides inside the cell (Table 1), albeit very close to the canalicular membrane (Figure 1A). Using immunofluorescence and confocal laser scanning microscopy, the majority of immunoreactive Mrp2 is seen to lie within the two ZO-1 boundaries under normo-osmolar (results not shown) and hypo-osmolar (Figure 2B) conditions, whereas only a little Mrp2 was detectable in the pericanalicular area. The theoretical resolution of the confocal set-up used in our studies is 150 nm. Therefore Mrp2 molecules which co-localize with the fluorescent bands of ZO-1 cannot clearly be assigned to the canalicular membrane or the pericanalicular zone, as can be done with electron microscopy.

### Effects of ambient osmolarity on GS-DNP secretion

In the perfused rat liver, CDNB is easily taken up by parenchymal cells and conjugated with glutathione. The conjugation product GS-DNP is preferentially excreted into bile via Mrp2 [24]. When the osmolarity of the perfusion buffer was changed from hypo-osmolar to hyperosmolar in the same experiment, there was a rapid shift from a predominantly biliary excretion of GS-DNP to sinusoidal release. This effect was reversible after re-institution of hypo-osmolar buffer (Figure 3). Aniso-osmolarity had no effect on the rate of CDNB conjugation, as the sum of GS-DNP release into bile and perfusate remained constant.

The biliary secretion of GS-DNP before, during and after hyperosmolar perfusion (in the steady-state phases) was $25.9 \pm 2.0$, $19.9 \pm 2.7$ and $27.3 \pm 3.7$ nmol/min per g of liver respectively. Thus hyperosmolar perfusion reduced Mrp2 activity by approx. 27%. This corresponds well with the decrease in the relative amount of Mrp2 $[g_{bcm}/(g_{bcm}+g_{cyt})]$ from 53% (at 205 mosmol/l) to 37% (at 405 mosmol/l), which is a reduction of 30% $[1-(0.37/0.53)]$. This again supports the view of a direct functional effect of Mrp2 redistribution on excretory activity, and suggests that hyperosmolarity may have no or little effect on the activity of Mrp2 molecules that remain in the canalicular membrane.

### Selectivity of Mrp2 redistribution due to ambient osmolarity

In normo- or hypo-osmotically perfused livers, immunoreactive Mrp2 was localized almost exclusively in the canalicular membrane, as shown by confocal laser scanning microscopy (Figure 2B). In contrast, there was a shift of Mrp2 inside the cells, i.e. alongside the tight-junction protein ZO-1, under hyperosmotic conditions (Figure 2A). Interestingly, this shift seemed to be selective: in hypo-osmotically perfused livers Mrp2 and Dpp IV, another canalicular marker protein, completely co-localized in the canalicular membrane of hepatocytes (Figure 2D). In hyperosmotically perfused livers the canalicular domain still showed co-localization of Mrp2 and Dpp IV; however, the Mrp2 retrieved into the cell did not co-localize with DppIV (Figure 2C). Similar findings were reported following LPS treatment: again Mrp2, but not DppIV, was retrieved from the canaliculi [11]. This selectivity is supported by the electron-microscopy findings, in that no changes in the morphometric parameters (surface and volume of the bile canaliculi) were observed under hyperosmolar perfusion or following LPS treatment.

The process of hyperosmotic Mrp2 retrieval was reversible at the level of function (Figure 3) when hypo-osmolarity was re-instituted. This is in line with observations of the re-insertion of Mrp2 shown by immunohistochemistry and confocal laser microscopy: 30 min after hyperosmolar perfusion Mrp2 was partly localized inside the cells (Figures 2A and 2C), while hypo-osmolar perfusion of the same livers led to relocalization of Mrp2 in the canalicular membrane (Figures 2B and 2D, and [13]).

Likewise, treatment of rat livers with LPS led to marked down-regulation of Mrp2 activity [11], which was reversible at early stages of LPS treatment [11]. This reversibility makes it unlikely that loss of Mrp2 from the canalicular membrane occurs via a significant expulsion of transporter molecules into bile.

### Conclusions

In summary, hyperosmolarity and LPS treatment induce a retrieval of Mrp2 from the canalicular membrane into the cytosol without significantly affecting the morphology of the canaliculi at the electron-microscopic level. Quantitative assessment of the amount of Mrp2 retrieved due to hyperosmolarity or LPS agrees well with the accompanying decline in Mrp2 function, as assessed by GS-DNP excretion in the perfused liver. Thus the effects of hyperosmolarity and LPS on the excretion of Mrp2 substrates can be largely explained by carrier retrieval.

This study was supported by the Deutsche Forschungsgemeinschaft through grants Ha 1160/6-3/6-4, the Sonderforschungsbereich 503 Düsseldorf and Do 622/1-3.

## REFERENCES


1 Keppler, D. and König, J. (1997) Expression and localization of the conjugate export pump encoded by the MRP2 (cMRP/cMOAT) gene in liver. FASEB J. **11**, 509–516
2 Müller, M. and Jansen, L. M. (1997) Molecular aspects of hepatobiliary transport. Am. J. Physiol. **272**, G1285–G1303
3 Meier, P. J. (1995) Molecular mechanisms of hepatic bile salt transport from the sinusoidal blood into bile. Am. J. Physiol. **268**, G801–G812
4 Müller, M. and Jansen, P. L. M. (1998) The secretory function of the liver: new aspects of hepatobiliary transport. J. Hepatol. **28**, 344–354
5 Paulusma, C. C., Bosma, P. J., Zaman, G. J. R., Bakker, C. T. M., Otter, M., Scheffer, G. L., Scheper, R. J., Borst, P. and Oude-Elferink, R. P. J. (1996) Congenital jaundice in rats with a mutation in a multidrug resistance-associated protein gene. Science **271**, 1126–1128
6 Büchler, M., König, J., Brom, M., Kartenbeck, J., Spring, H., Horie, T. and Keppler, D. (1996) cDNA cloning of the hepatocyte canalicular isoform of the multidrug resistance protein, cMRP, reveals a novel conjugate export pump deficient in hyperbilirubinemic mutant rats. J. Biol. Chem. **271**, 15091–15098
7 Taniguchi, K., Wada, M., Kohno, K., Nakamura, T., Kawabe, T., Kawakami, M., Kagotani, K., Okumura, K., Akiyama, S. and Kuwano, M. (1996) A human canalicular multispecific organic anion transporter (cMOAT) gene is overexpressed in cisplatin-resistant human cancer cell lines with decreased drug accumulation. Cancer Res. **56**, 4124–4129
8 Trauner, M., Meier, P. J. and Boyer, J. L. (1998) Molecular pathogenesis of cholestasis. N. Engl. J. Med. **339**, 1217–1227
9 Kartenbeck, J., Leuschner, U., Mayer, R. and Keppler, D. (1996) Absence of the canalicular isoform of the MRP gene-encoded conjugate export pump from the hepatocytes in Dubin-Johnson Syndrome. Hepatology **23**, 1061–1066
10 Trauner, M., Arrese, M., Soroka, C. J., Meenakshisundaram, A., Koeppel, T. A., Schlosser, S., Suchy, F. J., Keppler, D. and Boyer, J. L. (1997) The rat canalicular conjugate export pump (Mrp2) is downregulated in intrahepatic and obstructive cholestasis. Gastroenterology **113**, 255–264
11 Kubitz, R., Wettstein, M., Warskulat, U. and Häussinger, D. (1999) Regulation of the multidrug resistance protein 2 in the rat liver by lipopolysaccharide and dexamethasone. Gastroenterology **116**, 401–410
12 Kubitz, R., Warskulat, U., Schmitt, M. and Häussinger, D. (1999) Dexamethasone- and osmolarity-dependent expression of the multidrug resistance protein 2 in cultured rat hepatocytes. Biochem. J. **340**, 585–591
13 Kubitz, R., D'Urso, D., Keppler, D. and Häussinger, D. (1997) Osmodependent dynamic localization of the multidrug resistance protein 2 in the rat hepatocyte canalicular membrane. Gastroenterology **113**, 1438–1442
14 Rost, D., Kartenbeck, J. and Keppler, D. (1999) Changes in the localization of the rat canalicular conjugate export pump MRP2 in phalloidin-induced cholestasis. Hepatology **29**, 814–821
15 Stevenson, B. R., Siliciano, J. D., Mooseker, M. S. and Goodenough, D. A. (1986) Identification of ZO-1: a high molecular weight polypeptide associated with the tight junction (zonula occludens) in a variety of epithelia. J. Cell Biol. **103**, 755–766
16 Becker, A., Neumeier, R., Heidrich, C., Loch, N., Hartel, S. and Reutter, W. (1986) Cell surface glycoproteins of hepatocytes and hepatoma cells identified by monoclonal antibodies. Biol. Chem. Hoppe Seyler **357**, 681–688
17 Häussinger, D., Hallbrucker, C., Saha, N., Lang, F. and Gerok, W. (1992) Cell volume and bile acid secretion. Biochem. J. **288**, 681–689
18 Häussinger, D., Saha, N., Hallbrucker, C., Lang, F. and Gerok, W. (1993) Involvement of microtubules in the swelling-induced stimulation of transcellular taurocholate transport in perfused rat liver. Biochem. J. **291**, 355–360
19 Noé, B., Schliess, F., Wettstein, M., Heinrich, S. and Häussinger, D. (1996) Regulation of taurocholate excretion by a hypoosmolarity-activated signal transduction pathway in rat liver. Gastroenterology **110**, 858–865
20 Wahlländer, A. and Sies, H. (1979) Glutathione S-conjugate formation from 1-chloro-2,4-dinitrobenzene and biliary S-conjugate excretion in the perfused rat liver. Eur. J. Biochem. **96**, 441–446
21 Akerboom, T. P. M. and Sies, H. (1989) Transport of glutathione, glutathione disulfide and glutathione conjugates across the hepatocyte plasma membrane. Methods Enzymol. **173**, 523–534
22 Weibel, E. R. (1969) Stereological principles for morphometry in electron microscopy. Int. Rev. Cytol. **26**, 235–302
23 Jansen, P. L., Groothuis, G. M., Peters, W. H. and Meijer, D. F. (1987) Selective hepatobiliary transport defect for organic anions and neutral steroids in mutant rats with hereditary-conjugated hyperbilirubinemia. Hepatology **7**, 71–76
24 Oude-Elferink, R. P. J., Ottenhoff, R., Liefting, W., De Haan, J. and Jansen, P. L. M. (1989) Hepatobiliary transport of glutathione and glutathione conjugate in rats with hereditary hyperbilirubinemia. J. Clin. Invest. **84**, 476–483


Received 15 December 1999/7 February 2000; accepted 9 March 2000